Eur Biophys J (1998) 27: 197–209

ARTICLE

S. Svetina · B. Žekš · R. E. Waugh · R. M. Raphael

Theoretical analysis of the effect of the transbilayer movement of phospholipid molecules on the dynamic behavior of a microtube pulled out of an aspirated vesicle

Received: 29 November 1996 / Revised version: 1 December 1997 / Accepted: 9 January 1998

Abstract Observations over extended times of a lipid microtube (tether) formed from a lecithin vesicle have shown that under constant external loads the tether exhibits a continuous slow growth. It is considered that this growth is a consequence of the net transbilayer movement of phospholipid molecules in a direction which relieves the membrane strain resulting from the elastic deformation of the vesicle. The elastic deformation mode responsible for this effect is identified as the relative expansion of the two membrane layers reflecting the non-local contribution to membrane bending. An equation for the consequent rate of transbilayer movement of phospholipid molecules is derived. The dynamic behavior of the system is modeled by including frictional contributions due to interlayer slip and Stokes drag on the glass bead used to form the tether. The general numerical solution reveals a complex dependence of the tether growth rate on the system parameters and a continuous increase in the rate of tether growth at long times. Closed form expressions approximating the system behavior are derived and the conditions under which they can be applied are specified. Modeling the mechanically-driven lipid transport as a simple, stochastic, thermal process, allows the rate of lipid translocation to be related to the equilibrium transbilayer exchange rate of phospholipid molecules. Consideration of experimental results shows that the time constant for mechanically-driven translocation is shorter than the time for diffusion-driven translocation by approximately two orders of magnitude, indicating that lipid translocation is not a simple diffusive process.

Key words Membrane microtubes · Membrane elasticity · Phospholipid translocation

S. Svetina (✉)[1] · B. Žekš
Institute of Biophysics, Medical Faculty,
University of Ljubljana, and J. Stefan Institute,
1105 Ljubljana, Slovenia

R. E. Waugh
Department of Pharmacology and Physiology,
University of Rochester School of Medicine and Dentistry,
Rochester, NY 14642, USA

R. M. Raphael
Department of Biomedical Engineering, Johns Hopkins University
School of Medicine, Baltimore, MD 21205, USA

Corresponding address:
[1] Institute of Biophysics, Medical Faculty, University of Ljubljana,
Lipičeva 2, 1105 Ljubljana, Slovenia
(e-mail: sasa.svetina@biofiz.mf.uni-lj.si)

Introduction

A number of cellular processes involve deformation of membrane bilayers and the formation of small vesicles or tubo-vesicular structures. Studies of the mechanical properties of thin membrane tubes are invaluable for understanding such processes in which membranes and membrane deformation play an active role. In addition, formation of thin membrane microtubes (tethers) from bilayer membranes under well controlled conditions provides a powerful physical approach for investigating the fundamental elastic and dynamic properties of lipid bilayers. In previous studies tether formation has been used to determine the local and non-local bending constants of phospholipid bilayer membranes (Waugh et al. 1992), the coefficient of interleaflet friction (Evans and Yeung 1994), the apparent rate of interleaflet lipid transport (Raphael and Waugh 1996), as well as the role of the red cell membrane skeleton in stabilizing the red cell bilayer (Waugh and Bauserman 1995). In the interpretation of these experiments it is important to use a reliable theoretical approach. Inevitably, mechanical analyses of tether formation experiments involve some simplifying assumptions. As the experimental methodology has developed, a number of these assumptions have been challenged, and the models used to interpret the experimental outcome have continued to evolve.

The particular approach to tether formation being addressed in the present analysis was first introduced by Bo and Waugh (1989). A vesicle was aspirated into a pipette forming a spherical portion outside the pipette and a projection within the pipette. A glass bead was attached to the spherical portion of the vesicle opposite the pipette, and a

tether was pulled out of the surface as a consequence of the gravitational force on the bead. An equilibrium configuration of the tethered vesicle can be established at a particular pipette aspiration pressure for a given weight of the bead. This equilibrium is characterized by a tether of a certain radius and a certain length, and also depends on the values of the membrane local and non-local bending moduli (Božič et al. 1992). Measurements of the tether length and the length of the vesicle projection within the pipette as a function of the aspiration pressure can be used to determine these two bending moduli (Waugh et al. 1992).

Subsequent to these initial studies on the elastic properties of bilayer membranes, attention was focused on the dynamic aspects of tether formation. In one set of experiments the response of the system to a step decrease of the aspiration pressure was observed. The system was found to relax to the new equilibrium state by a time delay which can be ascribed to the fluid drag on the moving bead and the drag at the interface between the leaflets of the bilayer (Evans et al. 1992). The latter drag has also been shown to be important in the determination of the dispersion relation for a fluid bilayer membrane (Seifert and Langer 1993). Evans and Yeung (1994) performed a detailed analysis of the kinematics of the bilayer as it flows from the body of the vesicle onto the tether. Their solution provides information about the time dependent distribution of area strain in the two leaflets of the membrane as the tether grows and formed the basis for obtaining the interleaflet drag coefficient from the experimental data. The analysis predicts that after a step reduction in the aspiration pressure, the system should approach a new equilibrium state on an exponential time course, the time constant of which contains the interleaflet drag coefficient.

Further refinements in the experimental approach (Raphael and Waugh 1996) made it possible to study the behavior of the system over extended times. Careful observation of the length of the tether after a step reduction in aspiration pressure revealed the surprising result that the system does not reach a true equilibrium but that the tether continues to grow at a slow rate. The unrealized expectation that a new equilibrium should be reached was based on the knowledge that as the tether length increases, the difference in areas between the leaflets of the bilayer increases proportionately. If the number of molecules in each leaflet remains constant, this would result in an elastic deformation of the two membrane leaflets and an increase in the energy of the system due to the non-local bending elasticity of the membrane. That an equilibrium was not reached indicated that the non-local elasticity was relaxing, possibly as a result of a net movement of molecules from the compressed inner leaflet of the bilayer to the expanded outer leaflet. The original analysis of Yeung and Evans (1994) was extended to include a relaxation of the difference in area strain between the leaflets by a transport of molecules between leaflets (lipid translocation) (Raphael and Waugh 1996). (This generalized model was originally proposed by Evans (Evans et al. 1992) but the coefficient for interleaflet transport was taken to be zero in his subsequent analyses.) To obtain the solution to this problem, a number of simplifying assumptions were made, notably, that the vesicle consisted simply of a sphere with constant radius and that the membrane tension (isotropic force resultant) in the body of the vesicle was constant while the tether was being pulled out. The prediction of this extended analysis is that the tether length should increase in time as the sum of an exponential plus a linear term. The three free parameters of the fit were used to obtain the interleaflet drag coefficient, the non-local bending elastic modulus and the coefficient characterizing the rate of lipid translocation.

In the present work a different analytical approach is used to obtain a prediction of the time course of tether formation after a step reduction in aspiration pressure. It follows the hypothesis that the long term growth of the tether is a reflection of a net movement of lipid molecules between the leaflets of the bilayer. This movement is ascribed to be the consequence of a driving force which results from differential changes in the area density of phospholipid molecules in the two membrane monolayers induced during tether formation (Božič et al. 1992). The corresponding theoretical analysis is based on a description of the free energy of the vesicular phospholipid membrane that includes as a parameter the difference between the equilibrium areas of the two bilayer leaflets (Svetina et al. 1985). Because this difference is proportional to the difference between the number of molecules in these leaflets, the free energy of the system can decrease by the net transbilayer movement of phospholipid molecules. The model is designed to be technically tractable but complete in the sense that it takes into consideration all the factors which are known to affect the behavior of the system. In particular, the model reproduces the system geometry quite closely and accounts for both elastic and dissipative contributions to the energy. One simplifying assumption is that the distribution of area strain is uniform over the vesicle surface. This assumption is supported by the analysis of Raphael and Waugh (1996) in which it is shown that spatial gradients in the area strain dissipate rapidly over the surface of the vesicle, such that for most of the time during which the tether is formed, the distribution of strain is uniform except for a small region very near the tether. As will be shown, the prediction that the time course of tether growth should be the sum of an exponential plus a linear term is recovered in certain limiting cases, and the conditions under which this approximation is valid are precisely defined. In addition, a rational thermodynamic basis for comparing the apparent rate of lipid translocation in tether experiments with half times of lipid exchange measured by other methods is provided.

Elastic properties of phospholipid bilayers and vesicle shapes

Phospholipid bilayer membranes are composed of two layers which can in many instances be considered as independent physical entities because the transbilayer move-

ment of phospholipids is slow. This slowness is the reflection of phospholipid exchange halftimes which are of the order of hours and days (Wimley and Thompson 1991). The two layers are held in close contact by the hydrophobic effect and therefore their areas are related by the expression:

$$A^{out} = A^{in} + h \int (c_1 + c_2)\, dA\,, \qquad (1)$$

where A^{out} and A^{in} are the areas of the neutral surfaces of the outer and the inner layer, respectively, h is the distance between these surfaces, and c_1 and c_2 are the two principal curvatures. Integration is over the membrane area ($A \cong A^{out} \cong A^{in}$) of the vesicle.

Although in contact, the two layers of a phospholipid bilayer can move laterally over each other and therefore are able to relax their elastic strains independently. Consequently, the elastic energy of a bilayer is essentially the sum of the elastic energies of the two layers. By considering that each layer behaves in the plane of the membrane as a two-dimensional liquid and that it has the properties of an elastic body if it is bent, the elastic energy of a bilayer can, by also taking into consideration the relationship 1, be expressed as a sum of the membrane area expansivity term, the non-local bending term, and the bending term (Evans 1980; Svetina et al. 1985; Božič et al. 1992; Miao et al. 1994; Svetina and Žekš 1996). This sum reads, with its individual terms written in the indicated order, as

$$W_{el} = \frac{1}{2}\frac{K}{A_0}(A - A_0)^2 + \frac{1}{2}\frac{k_r}{A_0 h^2}(\Delta A - \Delta A_0)^2 + \frac{1}{2} k_c \int (c_1 + c_2 - c_0)^2\, dA\,. \qquad (2)$$

Here A is the area of the bilayer neutral surface, A_0 the corresponding unstretched area and K the area expansivity modulus. ΔA is the difference between the areas of the two membrane monolayers ($A^{out} - A^{in}$), ΔA_0 the corresponding equilibrium difference ($A_0^{out} - A_0^{in}$), and k_r the non-local bending modulus. In the last term, k_c is the local bending modulus, c_0 the spontaneous curvature (Helfrich 1973), and integration extends over the whole membrane area.

A free phospholipid vesicle is expected to assume an equilibrium shape which corresponds to the minimum of the elastic energy, Eq. (2). The theoretical equilibrium shape can be obtained by variational methods where the equilibrium membrane area A_0, equilibrium area difference (ΔA_0), the spontaneous curvature (c_0), and in many applications also vesicle volume (V) are given (Svetina and Žekš 1989, Heinrich et al. 1993). In the case that forces are applied to the vesicle, the functional to be minimized to obtain the equilibrium vesicle shape is the system free energy, which also includes the potential energy due to the work done by the applied forces (Božič et al. 1992).

The non-local bending term in Eq. (2) is the direct measure of the energy contribution due to the difference in the area density of molecules in the two membrane leaflets. The difference $\Delta A - \Delta A_0$, and thus the non-local bending contribution to the elastic energy of the vesicle have a non-zero value in a phospholipid vesicle when the areas A^{out} and A^{in} are not in the relaxed state, i. e. in the state in which each individual layer would have the minimum elastic energy corresponding to the respective equilibrium areas A_0^{out} and A_0^{in}. The difference $\Delta A - \Delta A_0$ can be particularly pronounced under experimental conditions which cause a drastic change of the vesicle shape, such as during tether formation experiments.

For a vesicle with a membrane composed of a single component the equilibrium area difference ΔA_0 can be expressed in terms of the numbers of molecules in the outer (N^{out}) and the inner (N^{in}) layer, and the corresponding areas per molecule in the relaxed monolayer state ($\bar{A}_0^{out}$ and $\bar{A}_0^{in}$).

$$\Delta A_0 = N^{out}\bar{A}_0^{out} - N^{in}\bar{A}_0^{in} \qquad (3)$$

It is clear that by the transbilayer transfer of molecules the equilibrium area difference ΔA_0 is changed, and that by this process the non-local bending contribution to the elastic energy can be decreased.

Relaxation of non-local bending elasticity during tether formation

The free energy in the tether pulling experiment is obtained sufficiently accurately (Božič et al. 1992, 1997) by simulating the shape of a vesicle as a geometrical body described in terms of a relatively small set of parameters, by ascribing to this shape the membrane elastic energy, and by including the contributions due to the external forces. We consider a geometrical body (Fig. 1) where the part of the vesicle inside the pipette is described as a cylinder with the radius of the internal surface of the pipette wall (R_p) ending with a hemispherical cap of the same radius. The length of the projection within the pipette is denoted by L_p. The vesicle outside the pipette is described by a sphere with radius R_v. The tether is assumed to be a cylinder with radius R_t and length L_t. For a given pipette there are, in this model, four free geometrical parameters. They are interrelated because the vesicle volume is constant, and (it is assumed) the membrane is laterally incompressible at the bilayer neutral surface, such that the vesicle area is also constant ($A = A_0$). Because the tether radius is small, the

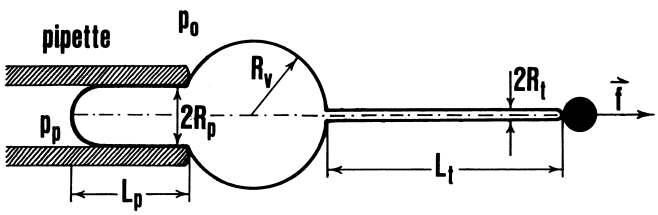

Fig. 1 Schematic representation of the vesicle which is aspirated in a pipette and pulled with constant force (f) in the opposite direction. The shape is described by one parameter (R_p) and four variables (tether length L_t, tether radius R_t, pipette projection length L_p, and vesicle radius R_v). The pressure surrounding the vesicle is p_0, and the pressure in the pipette is p_p

volume of the tether can be neglected, and the volume of the vesicle (V) is given nearly exactly by the volume of the pipette part plus the outside spherical part of the vesicle,

$$V = -\frac{\pi}{3} R_p^3 + \pi L_p R_p^2 + \frac{4\pi}{3} R_v^3 . \quad (4)$$

The vesicle area (A_0) in the model is equal to

$$A_0 = -\pi R_p^2 + 2\pi L_p R_p + 4\pi R_v^2 + 2\pi L_t R_t . \quad (5)$$

To predict quantitatively the tether behavior it is sufficient to include in the expression of the free energy (F) of the described model only the significant energy contributions. This gives

$$F = 2\pi^2 k_r (L_t - L_t^*)^2 / A_0 + \pi k_c \frac{L_t}{R_t} - f L_t - \Delta p \pi R_p^2 L_p + \Delta\sigma\, 2\pi R_p (L_p - R_p) , \quad (6)$$

where f is the tether pulling force, Δp the aspiration pressure (pressure in the outside solution minus the pressure in the pipette) and $\Delta\sigma$ the difference between the surface energies of membrane/glass and membrane/outside solution interfaces. In the first term, which is the relative expansivity term, the area difference ΔA is expressed in terms of the tether length L_t so that

$$L_t = (\Delta A - \Delta A_i)/2\pi h \quad (7)$$

where ΔA_i is the area difference of the aspirated and spherical part of the vesicle. Correspondingly, the equilibrium area difference ΔA_0 and the related contribution due to the spontaneous curvature c_0 are replaced by the hypothetical tether length L_t^* defined as

$$L_t^* = (\Delta A_0 + k_c A_0 h^2 c_0/k_r - \Delta A_i)/2\pi h \quad (8)$$

It was recognized (Božič et al. 1992) that the changes of the area difference ΔA_i are negligible in comparison to the area difference variation due to changes of tether length and therefore ΔA_i in Eq. (8) can be considered as a constant. In the local bending term (the second term on the right hand side of Eq. (6), it is also sufficient to include only the contribution from the tether. The third term in Eq. (6) is the gravitational potential energy of the bead, and the fourth term represents the work done owing to the pressure difference between the pressure in the pipette and the outside solution. The last term, which accounts for the altered environment of the part of the membrane in contact with the pipette wall, does not appear in expressions for the free energy used in previous publications (Božič et al. 1992), but has been added here for the sake of completeness, even though, as will be shown, in the examples to be treated its inclusion does not affect predictions of the tether dynamics.

To reveal the effects of different relaxation processes involved in the tether dynamics, we shall consider two separate examples. As transbilayer movement is expected to be a slow process in comparison with other processes through which the system approaches a new equilibrium after alteration of the external forces, we shall first assume that for a given value of ΔA_0 (or L_t^*) the system is always in its elastic equilibrium, i. e. the vesicle assumes the conformation corresponding to the minimum of the free energy, Eq. (6), at the unchanged ΔA_0 value. In this way, the effect of phospholipid transmembrane movement on the tether dynamics can be revealed independently of other relaxation effects that may influence tether dynamics during the transition between equilibrium states. For instance, we neglect the interlayer drag. The latter will be included in the second example in which it will not be assumed a priori that the tether length is an equilibrated parameter.

Flip-flop relaxation for an elastically equilibrated tether

For a given Δp, the equilibrium tether configration for a vesicle of a given membrane area, volume and the equilibrium area difference ΔA_0 (or L_t^*), can be determined by equating to zero the derivatives of the free energy F (Eq. (6)) by the free variables of the system (Božič et al. 1992). These are conveniently chosen to be L_t and R_v. The pipette projection length L_p can be eliminated using the volume conservation equation: from Eq. (4) we obtain

$$L_p = L_{p,0} + \frac{4}{3R_p^2}(R_{v,0}^3 - R_v^3) , \quad (9)$$

with the index "0" denoting the parameter values of the initial state of the system when the tether is just formed and its length ($L_{t,0}$) is still negligible. Furthermore, the tether radius R_t can be eliminated from the area conservation equation Eq. (5), which, by taking into consideration Eq. (9) and when reexpressed, reads

$$\frac{1}{R_t} = \frac{L_t}{L_{t,0} R_{t,0} - 4(R_{v,0}^3 - R_v^3)/3R_p + 2(R_{v,0}^2 - R_v^2)} . \quad (10)$$

Then the equilibrium equations which are obtained by setting to zero the partial derivatives of Eq. (6) by L_t and R_v, respectively, are

$$\frac{4\pi^2 k_r}{A_0}(L_t - L_t^*) + \frac{2\pi k_c}{R_t} - f = 0 , \quad (11)$$

and

$$\Delta p - \frac{2\Delta\sigma}{R_p} - \frac{k_c}{R_t^2}(1/R_p - 1/R_v) = 0 . \quad (12)$$

In the tether pulling experiment we are interested in the tether behavior of the system after the tether is already formed. Therefore Eq. (12) can be replaced by the difference between this equation and the same equation for the initial tether with the practically zero tether length $L_{t,0}$, the radius $R_{t,0}$, the vesicle radius $R_{v,0}$, and the projection length $L_{p,0}$. This replacement is also convenient because the parameter $\Delta\sigma$ which is not pertinent for the dynamical behavior of the tether does not enter the equations. Then we have instead of Eq. (12)

$$\Delta p_r - \frac{k_c}{R_t^2}(1/R_p - 1/R_v) + \frac{k_c}{R_{t,0}^2}(1/R_p - 1/R_{v,0}) = 0 , \quad (13)$$

where Δp_r is the difference between a given aspiration pressure and the aspiration pressure at the initial state (Δp_0).

Assuming that at a given ΔA_0 (or L_t^*) all system parameters have already attained their equilibrium values, the tether dynamics can be described approximately by the following relationship

$$\frac{dL_t^*}{dt} = -\Gamma \frac{\partial F}{\partial L_t^*}, \tag{14}$$

where Γ is a phenomenological kinetic coefficient (Landau and Khalatnikhov 1954). Using Eq. (6) for the free enery, one obtains

$$\frac{dL_t^*}{dt} = \Gamma \frac{4\pi^2 k_r}{A_0}(L_t - L_t^*) = \frac{1}{\tau_p}(L_t - L_t^*), \tag{15}$$

where the characteristic time τ_p is given by

$$\tau_p = \frac{A_0}{\Gamma 4\pi^2 k_r}. \tag{16}$$

The dynamic behavior of the system can be calculated from Eq. (15) by substituting for the value of L_t the value obtained by solving Eqs. (10), (11) and (13) for the instantaneous value of the difference between the areas of the two membrane layers, represented by the parameter L_t^*. In integral form, Eq. (15) can be written as

$$\int_{L_{t,0}^*}^{L_t^*} \frac{dL_t^*}{L_t(L_t^*) - L_t^*} = \frac{t}{\tau_p}. \tag{17}$$

The direct result of integrating Eq. (17) is the value of L_t^* at time t; however, the values of the vesicle parameters L_t, R_t and R_v at this time are also obtained. In addition, the value of the pipette projection length L_p can be calculated by substituting the value of R_v into Eq. (9). It must be noted that because L_t^* appears only in Eq. (11) and not in Eqs. (10) and (13), the values of the vesicle parameters R_t, R_v and L_p can be written as expressions which contain only L_t; that is, the values of R_t, R_v and L_p can be known without knowing the value of L_t^*. This means that the relationships among the four geometrical vesicle parameters are not affected by the dynamic features of the system.

It is instructive to visualize the behavior of the system as predicted by these model equations. The result of the integral, Eq. (17), depends on the initial value of L_t^*, i.e. on $L_{t,0}^*$ which depends on the vesicle history and is in principle unknown. Therefore we make an assumption that the system is initially equilibrated in the sense that the hypothetical tether length (Eq. (8)) becomes equal to the actual tether length, meaning that $L_{t,0}^* = L_{t,0}$. Such an equilibration can be realized experimentally by observing the tether length L_t and keeping it fixed over a long time by continuously adjusting the aspiration pressure until it becomes constant. In the case of constant tether length it follows from Eq. (15) that L_t^* approaches the value $L_{t,0}$ ($\cong 0$) on an exponential time course with the characteristic time constant τ_p.

This situation is realized experimentally whenever after a tether grows for a long time it is returned to a very short length by simply increasing the suction pressure in the pipette. At the time the tether reaches a short length it still "wants" to be longer because of the relative increase in the number of molecules in the outer leaflet that occurred during the preceding pull. Consequently, the pressure required to maintain the tether at a short constant length is at first greater than the initial equilibrium pressure (Δp_r is positive), and then decreases over time in accordance with the decrease in L_t^*. The time dependence of the pressure difference Δp_r during this period can be obtained from the equilibrium Eqs. (11) and (13) by setting $L_t = 0$ and putting $R_v = R_{v,0}$ (The latter follows from the requirement of constant area, Eq. (10). By eliminating R_t, the expression for Δp_r becomes

$$\Delta p_r = \frac{2 f k_r}{A_0 k_c} L_t^* \left(1 + \frac{2\pi^2 k_r}{f A_0} L_t^*\right)(1/R_p - 1/R_{v,0}). \tag{18}$$

Thus, during the relaxation of non-local elasticity at constant, approximately zero tether length, and for small enough values of L_t^* when the L_t^{*2} term in Eq. (18) can be neglected ($L_t^* \simeq 100$ μm), the pressure difference Δp_r also approaches the value zero on an exponential time course with time constant τ_p (see Fig. 2 for an experimental example).

Next we give the theoretical prediction of the tether growth experiment in which initially the tether is very short with the length $L_{t,0} \cong 0$. It is assumed that the system is equilibrated in the sense described above, so that initially

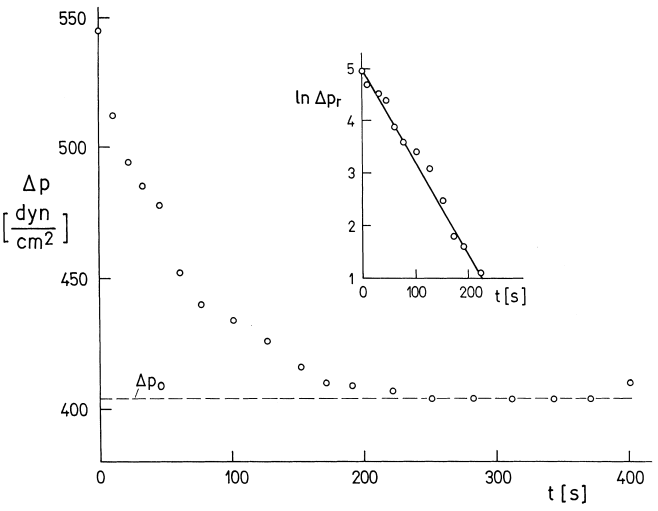

Fig. 2 The relaxation of the holding pressure as a function of time after returning a tether to a short length. After forming a tether approximately 600 μm in length, the aspiration pressure in the holding pipette was increased to withdraw the tether back onto the body of the vesicle. As the tether reached a very short length, the pressure was continuously adjusted to maintain a constant tether length. Points represent measured values of the pressure as a function of time. As expected (Eq. (18)), the pressure decreased on an exponential time course approaching the pressure difference Δp_0. The time constant for the fitted relaxation curve (the inset) is $\tau_p = 57$ s. Materials and methods are as in Raphael and Waugh (1996)

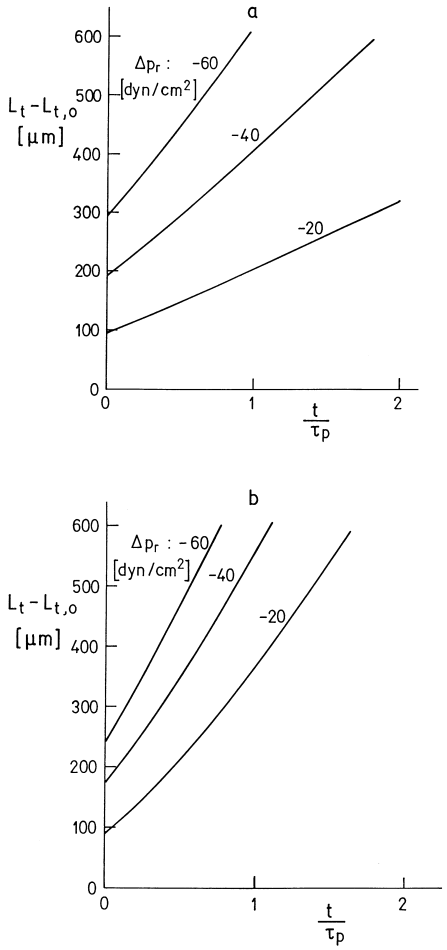

Fig. 3 a, b The time dependence of the tether length after the aspiration pressure is changed by the indicated amount (Δp_r) from the value at which the tether is equilibrated at nearly zero length ($L_{t,0} \simeq 0$) as predicted by Eq. (17) for the values of the local bending modulus $k_c = 1 \times 10^{-19}$ J and the ratio $k_r/k_c = 3$. It is assumed that at each value of L_t^* the tether parameters take their equilibrium values. Example (**a**) is a vesicle with $A_0 = 1123\ \mu m^2$, $V = 3014\ \mu m^3$, aspirated into the pipette with the radius $R_p = 4.01\ \mu m$ and strained by the force $f = 3.35\ \mu dyn$, yielding at chosen values of material constants the parameter $\alpha = 0.1$ (see Eq. (25)). Example (**b**) is a vesicle with $A_0 = 593\ \mu m^2$, $V = 1019\ \mu m^3$, aspirated into the pipette with the radius $R_p = 3.37\ \mu m$ and strained by the force $f = 5.30\ \mu dyn$, yielding at chosen values of material constants the parameter $\alpha = 0.62$

we have $L^*_{t,0} = L_{t,0} \cong 0$. The initial radius of the tether depends according to Eq. (11) on the applied force and the bending modulus k_c: $R_{t,0} = 2\pi k_c/f$. Then, at time zero, the aspiration pressure is instantaneously lowered, i. e., the value Δp_r is made negative. In accordance with the assumption of an immediate establishment of the tether equilibrium, after instantaneously lowering the aspiration pressure the system instantaneously increases its tether length and adjusts other geometrical parameters to values which correspond to the value Δp_r. After that the tether length increases according to Eq. (17). In Fig. 3 we show, for two vesicles exhibiting different experimental behavior (cf. Figs. 7 and 8), the time dependence of L_t predicted by choosing the values of the bending constants k_c and k_r, and assuming different instantaneous step changes in the values of the aspiration pressure (Δp_r). Initially, the tether length L_t has an approximately linear time dependence, the slope of which is larger for larger Δp_r values. At lower Δp_r values where the tether growth rate is smaller and the tether behavior can be followed for longer times, it can be noted that the tether length depends on time more strongly than linearly.

The behavior of the model depends on the values of the parameters of the system appearing in Eq. (17) and in Eqs. (9), (10), (11) and (13). To reveal the role of these different material, vesicle and experimental parameters in the tether dynamics it is useful to treat the dynamics analytically using different approximations. An appropriate approximation is obtained if from Eqs. (10) and (13) one eliminates the radius R_v and then expands the reciprocal tether radius ($1/R_t$) in terms of the change in tether length $L_t - L_{t,0}$ around its value ($1/R_{t,r}$) at $L_{t,0} \simeq 0$ which is

$$\frac{1}{R_{t,r}} = \left[\frac{1}{R_{t,0}^2} + \frac{\Delta p_r}{k_c \left(\frac{1}{R_p} - \frac{1}{R_{v,0}} \right)} \right]^{1/2} . \tag{19}$$

To first order, this expansion takes the form

$$\frac{1}{R_t} = \frac{1}{R_{t,r}} + \left. \frac{\partial \frac{1}{R_t}}{\partial L_t} \right|_0 (L_t - L_{t,0}) , \tag{20}$$

where, by neglecting the terms involving $L_{t,0}$,

$$\left. \frac{\partial \frac{1}{R_t}}{\partial L_t} \right|_0 = - \frac{1}{8 \left(\frac{1}{R_p} - \frac{1}{R_{v,0}} \right)^2 R_{v,0}^4} . \tag{21}$$

The radius of the vesicle is changing in this approximation as

$$R_v = R_{v,0} + \frac{R_{t,r}}{4 \left(\frac{1}{R_p} - \frac{1}{R_{v,0}} \right) R_{v,0}^2} (L_t - L_{t,0}) , \tag{22}$$

and consequently the pipette projection length is

$$L_p = L_{p,0} - \frac{R_{t,r}}{\left(\frac{1}{R_p} - \frac{1}{R_{v,0}} \right) R_p^2} (L_t - L_{t,0}) . \tag{23}$$

By inserting Eq. (20) into Eq. (11) the latter equation reads

$$-(L_t - L_t^*) + \beta + \alpha (L_t - L_{t,0}) = 0 , \tag{24}$$

where the constants α and β are

$$\alpha = \frac{k_c A_0}{16 \pi k_r \left(\frac{1}{R_p} - \frac{1}{R_{v,0}} \right)^2 R_{v,0}^4} \tag{25}$$

and

$$\beta = -\frac{k_c A_0}{2\pi k_r}\left(\frac{1}{R_{t,r}} - \frac{1}{R_{t,0}}\right), \tag{26}$$

where $1/R_{t,0} = f/2\pi k_c$ (Eq. (11)). The constant β at small values of Δp_r reduces to

$$\beta \simeq -\frac{k_c \Delta p_r A_0}{2 k_r f\left(\frac{1}{R_p} - \frac{1}{R_{v,0}}\right)}. \tag{27}$$

From Eq. (24) it is possible to obtain L_t and insert it into Eq. (17), which can then be integrated to yield

$$L_t^* = L_{t,0} + \frac{\beta}{\alpha}(e^{\lambda_2 t} - 1), \tag{28}$$

where

$$\lambda_2 = \frac{\alpha}{\tau_p (1-\alpha)}. \tag{29}$$

Finally

$$L_t = L_{t,0} + \frac{\beta}{1-\alpha} + \frac{\beta}{\alpha(1-\alpha)}(e^{\lambda_2 t} - 1). \tag{30}$$

The time dependence of L_t obtained using Eq. (30) is shown in Fig. 4 as the dashed lines.

For small times it is possible to expand the exponential function in Eq. (30) to give

$$L_t = L_{t,0} + \frac{\beta}{1-\alpha} + \frac{\beta}{(1-\alpha)^2}\frac{t}{\tau_p}. \tag{31}$$

This dependence is represented in Fig. 4 as the dotted lines. If the values of the parameter α, and consequently of λ_2 (see Eq. (29)), are sufficiently small the linear time course of L_t (Eq. (31)) may be valid throughout the experimental range of L_t.

In Fig. 4 the approximate predicted time dependence of the tether length L_t is compared to the exactly calculated dependence for two vesicles for which the values of the constant α (Eq. (25)) are significantly different. For smaller α the approximations introduced seem to be justified whereas at higher α they fail drastically. At large α, owing to the expansion of $1/R_t$, the approximation already deviates from the exact solution at $t = 0$ (Fig. 4, case b). For smaller values of α for which the approximations work, it is possible to visualize the role of different system parameters. The slope is essentially given by the ratio β/τ_p. It is thus under the validity of Eqs. (16) and (27) proportional to k_c and Δp_r, and inversely proportional to the force f. It does not depend on k_r. The initial increment of L_t on the other hand is proportional only to β (Eq. (26)) which means that it is also affected by the ratio k_r/k_c as was established previously in the corresponding equilibrium studies (Božič et al. 1992).

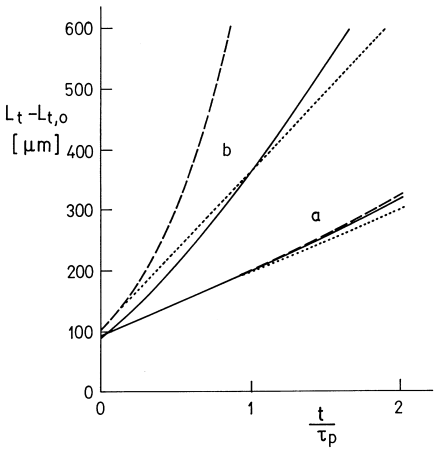

Fig. 4 The time dependence of the tether length after the aspiration pressure is changed by $\Delta p_r = -20$ dyn/cm^2 from the value at which the tether is equilibrated at nearly zero length ($L_{t,0} \simeq 0$) as predicted by Eq. (17) (*solid lines*), Eq. (30) (*dashed lines*), and Eq. (31) (*dotted lines*) for the values of the local bending modulus $k_c = 1\times10^{-19}$ J and the ratio $k_r/k_c = 3$, for the two vesicles with essentially different values of the parameter α (Eq. 25)). Vesicle a with $\alpha = 0.1$ is the example a from Fig. 3 whereas vesicle b with $\alpha = 0.62$ is the example b from Fig. 3

An effect of a frictional force proportional to the velocity of tether growth

There are at least two frictional contributions to the tether dynamics which are proportional to the velocity of the tether growth. These are the Stokes drag on the moving glass bead and the frictional dissipation within the membrane as it flows onto the tether. These contributions enter the present formulation as adjustments to the bead force on the tether. The contribution from the Stokes drag to the force takes the standard form:

$$f_{st} = 6\pi\eta R_b \, dL_t/dt, \tag{32}$$

where R_b is radius of the bead and η the viscosity coefficient. The viscous dissipation within the membrane is dominated by the frictional dissipation between leaflets as they flow at different rates from the cell body onto the tether. Because the area of the outer leaflet on the tether is greater than the area of the inner leaflet, the outer leaflet flows from the vesicle body with a higher velocity, generating a slippage between the leaflets at the midplane of the membrane. Evans and Yeung (1994) (see also, Hochmuth et al. 1996) presented the contribution to the tethering force from this mechanism in the form:

$$f_{lf} = 2\pi b h^2 \ln(R_v/R_t) \, dL_t/dt, \tag{33}$$

where b is the coefficient of the interlayer friction. Evans and Yeung (1994) define b simply as the constant of proportionality between the relative velocity between the two leaflets of the bilayer and the shear traction exerted by one layer on the other.

The force which drives the system towards equilibrium is, in this case, the derivative of the free energy by L_t, and it is opposed by the frictional force. The equation of mo-

tion for the bead is then:

$$4\pi^2 k_r (L_t - L_t^*)/A_0 + 2\pi k_c/R_t - f + c_s \, dL_t/dt = 0 , \quad (34)$$

with

$$c_s = 6\pi\eta R_b + 2\pi b h^2 \ln(R_v/R_t) . \quad (35)$$

In the simulations we shall consider the parameter c_s to be constant because the vesicle and tether radii R_v and R_t do not change appreciably. Equation (34) can be re-expressed as

$$\frac{dL_t}{dt} = \frac{1}{\tau_s}\left[-(L_t - L_t^*) - \frac{A_0}{4\pi^2 k_r}(2\pi k_c/R_t - f)\right], \quad (36)$$

where the characteristic relaxation time τ_s is given by

$$\tau_s = \frac{c_s A_0}{4\pi^2 k_r} . \quad (37)$$

Equations (36) and (15) form a set of differential equations which are to be integrated to obtain the time dependence of the tether length L_t and the area difference L_t^*. Here we neglect the effect of the lipid flip-flop on the equilibrium membrane area A_0 that directly affects L_t and makes the phenomenological frictional coefficient a non-diagonal matrix. Namely, for symmetric membranes $A_0 = 2N^{out} N^{in} \bar{A}_0/(N^{out} + N^{in})$ (Eq. (12) in Svetina et al. 1985, Eq. (A 18) in Miao et al. 1994)) from which it can be estimated that the relative contribution to the tether length due to the flip-flop induced change of A_0 is of the order of $(N^{out} - N^{in})/(N^{out} + N^{in})$, i. e. of the order of the ratio between the distance between the neutral surfaces of membrane monolayers (h) and the radius of the sphere with the area A_0. At each value of L_t and L_t^* the other parameters of the system are set to equilibrium. This means that

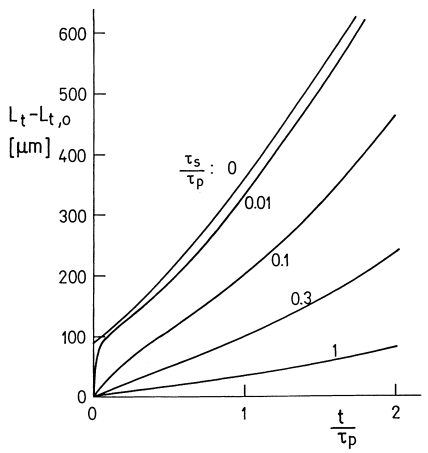

Fig. 5 The time dependence of the tether length after the aspiration pressure is changed for $\Delta p_r = -20$ dyn/cm^2 from the value at which the tether is equilibrated at nearly zero length, as predicted for the values of the ratio between the two relaxation times τ_s/τ_p which are given adjacent to the corresponding set of curves. The curve for $\tau_s/\tau_p = 0$ is obtained by integrating Eq. (17) whereas the other curves are obtained by integrating equations (15) and (36) by the Runge-Kutta method. It is assumed that at each set of values of L_t^* and L_t the remaining tether parameters assume their equilibrium values. Vesicle and system parameters are as in the example b in Fig. 3

Eq. (13) must be satisfied as well as the constraints (Eqs. (9) and (10)). The resulting time dependence of the tether length is shown in Fig. 5 for different values of the ratio τ_s/τ_p. At small values of this ratio (0.01) the predicted curve practically coincides with the corresponding one from the previous section, but at intermediate and higher values (0.1–1.0) significant deviations in the behavior of the tether are predicted. Physically, these differences are attributable to a reduction in the effective force on the tether due to viscous drag.

It is expected that for some vesicles it is possible to apply the analytical expressions for tether growth obtained when approximating the tether radius R_t by Eq. (20). Equation (36) can then be written as

$$\frac{dL_t}{dt} = \frac{1}{\tau_s}\left[-(L_t - L_t^*) + \beta + \alpha(L_t - L_{t,0})\right]. \quad (38)$$

Equations (38) and (15) describe the relaxational dynamical problem with a non-diagonal 2×2 dynamic matrix. By diagonalyzing it, the solution can be expressed as

$$L_t = -\frac{\beta}{\alpha} + \xi_1 e^{\lambda_1 t} + \xi_2 e^{\lambda_2 t} \quad (39)$$

and

$$L_t^* = -\frac{\beta}{\alpha} + \eta_1 e^{\lambda_1 t} + \eta_2 e^{\lambda_2 t} , \quad (40)$$

where

$$\lambda_1 = \frac{1}{2}\left\{-\left(\frac{1-\alpha}{\tau_s} + \frac{1}{\tau_p}\right) - \left[\left(\frac{1-\alpha}{\tau_s} + \frac{1}{\tau_p}\right)^2 + 4\frac{\alpha}{\tau_s \tau_p}\right]^{1/2}\right\} \quad (41)$$

$$\lambda_2 = \frac{1}{2}\left\{-\left(\frac{1-\alpha}{\tau_s} + \frac{1}{\tau_p}\right) + \left[\left(\frac{1-\alpha}{\tau_s} + \frac{1}{\tau_p}\right)^2 + 4\frac{\alpha}{\tau_s \tau_p}\right]^{1/2}\right\} \quad (42)$$

$$\xi_1 = -\frac{\beta}{\alpha}\frac{-\alpha + \tau_s \lambda_2}{\tau_s(\lambda_1 - \lambda_2)} \quad (43)$$

$$\xi_2 = \frac{\beta}{\alpha}\frac{-\alpha + \tau_s \lambda_1}{\tau_s(\lambda_1 - \lambda_2)} \quad (44)$$

$$\eta_1 = (1 - \alpha + \tau_s \lambda_1)\,\xi_1 \quad (45)$$

and

$$\eta_2 = (1 - \alpha + \tau_s \lambda_2)\,\xi_2 . \quad (46)$$

For $\tau_s \to 0$ Eq. (39) coincides with Eq. (30), and Eq. (42) coincides with Eq. (29). At times $t \ll \tau_p$ Eqs. (39) and (40) can be reduced to

$$L_t = \frac{\beta}{\tau_s} t \quad (47)$$

and

$$L_t^* = \frac{\beta}{2\tau_s \tau_p} t^2 . \quad (48)$$

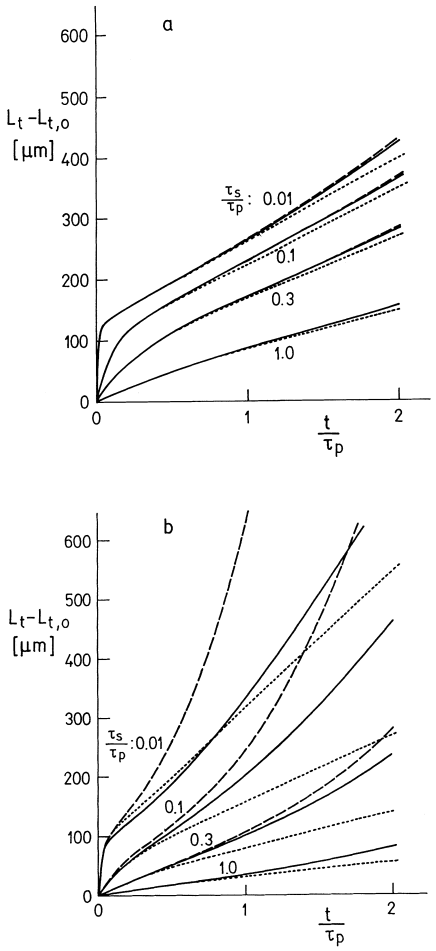

Fig. 6 a, b The comparison of the time dependence of the tether length after the aspiration pressure is changed for $\Delta p_r = -20$ dyn/cm^2 from the value at which the tether is equilibrated at nearly zero length, as predicted for the indicated values of the ratio between the two relaxation times τ_s/τ_p by integrating Eqs. (15) and (36) (*solid lines*), from Eq. (39) (*dashed lines*), and from Eq. (49) (*dotted lines*). Vesicle and system parameters in **a** and **b** are as in the examples a and b in Fig. 3

When the constant λ_s is sufficiently small the second exponential can be expanded and Eq. (39) simplified to

$$L_t = -\frac{\beta}{\alpha} + \xi_1 e^{\lambda_1 t} + \xi_2 + \xi_2 \lambda_2 t. \tag{49}$$

The criterion for the applicability of this approximation can be deduced from the requirement that the product $\lambda_2 t_{exp}$ (with t_{exp} the typical duration of the experiment) is smaller than a certain value ε such that the expansion of the exponential function can be terminated by the linear term. Then the parameter α must satisfy the inequality

$$\alpha < \frac{\varepsilon}{t_{exp}} \left(1 + \frac{\tau_s}{\tau_p}\right) \tag{50}$$

showing that the range of possible values of α for the approximation to be valid is larger at larger values of τ_s. This is illustrated in Fig. 6, in which it is shown that, for the same value of α, differences between the exact solution (integral of Eqs. (36) and (15)) and the approximate solutions (Eqs. (39) and (49)) are reduced for higher values of the ratio of τ_s/τ_p.

Analysis of experiments

The aim of this section is to illustrate the use of the derived expressions for tether dynamics to determine the membrane material constants. Two vesicles with qualitatively different dynamic behavior are treated. The measured parameters are the tether length L_t, the length of the vesicle projection in the pipette L_p and the aspiration pressure. The pressure is altered at the beginning of the experiment and is afterwards kept constant. The radius of the pipette, the radius of the bead and the bead density are measured separately.

The experimental results are the dependence of L_p on L_t and the time dependence of L_t. Over most of the tether length the relationship between L_t and L_p is linear. From the slope of the dependence of L_p on L_t (see Eq. (23)) it is possible to obtain k_c. From the time course of L_t one can then extract the values of k_r, τ_s and τ_p. In the determination of these parameters it is of advantage to employ the property of the system that the initial slope of the L_t time dependence which is (see Eq. (47))

$$\dot{L}_{t,0} = \beta/\tau_s \tag{51}$$

can be expressed only in terms of k_r and τ_s as unknowns. The fitting procedure may thus proceed as follows. By choosing the initial value of k_r in the expected range of values, the relaxation time τ_s is found via Eq. (51) using the measured value $\dot{L}_{t,0}$. The relaxation time τ_p is chosen in such a way that the predicted L_t time dependence passes a selected point of the experimental L_t time dependence. Then the value of k_r is varied until the predicted curve matches the experimental one over its whole measured range. An example of employing such a procedure is shown in Fig. 7.

When the system behaves according to Eq. (49) the procedure can be simplified by fitting the characteristic independent features of the $L_t(t)$ curve. For instance, these could be the initial slope of the L_t time dependence $\dot{L}_{t,0}$ (Eq. (51)), the slope of the asymptote which can be expressed as

$$\dot{L}_{t,\infty} = \xi_2 \lambda_2 \tag{52}$$

and its extrapolated value at time $t=0$ which can be expressed (see Eq. (49)) as

$$\Delta L_{t,e} = -\frac{\beta}{\alpha} + \xi_2 . \tag{53}$$

By introducing for the sake of a short notation $\gamma = \dot{L}_{t,0}/\dot{L}_{t,\infty}$ and $\delta = \alpha \Delta L_{t,e}/\beta$ (note that the ratio α/β only depends on the material parameter k_c), one can by some manipulations

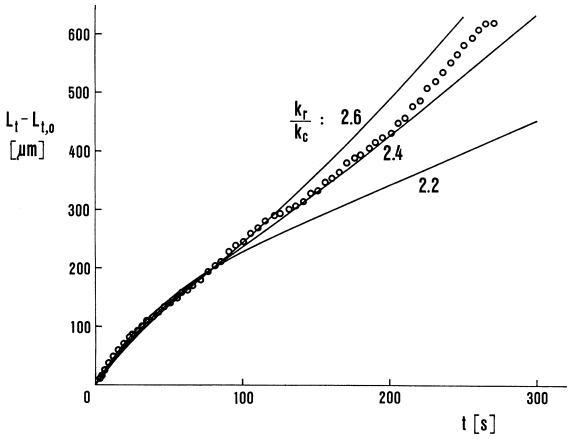

Fig. 7 An example of an analysis of the tether pulling experiment based on an integration of Eqs. (15) and (36). The predicted time dependences of the tether length (L_t) are compared to the data on a vesicle with a high value of the parameter α (vesicle b from Fig. 3). The dots are experimental values. The change of the aspiration pressure is $\Delta p_r = -21.4$ dyn/cm^2. The measured slope dL_p/dL_t (not shown) is -0.0143 which gives by employing Eq. (23) the local bending modulus $k_c = 1.1\times10^{-12}$ erg. The full lines represent the predicted L_t time dependence. The two parameters (τ_s and τ_p) are chosen so that the initial slope is equal to the experimental one and that the curve passes the experimental L_t value at t = 80 s. The three curves represent the predicted behavior of the system at three different values of the ratio k_r/k_c. The closest fit is obtained with $k_r/k_c = 2.4$, $\tau_s = 17$ s and $\tau_p = 190$ s. Materials and methods are as in Raphael and Waugh (1996)

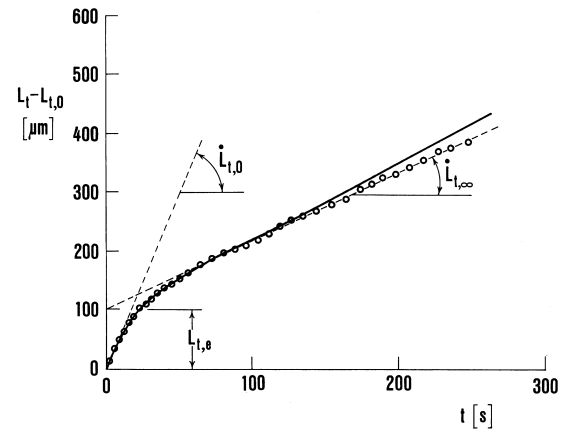

Fig. 8 An example of an analysis of the tether pulling experiment for the case of a vesicle for which the time dependence of the tether length (L_t) can be approximated by Eq. (49) (vesicle a from Fig. 3). The dots are experimental values. The change of the aspiration pressure is $\Delta p_r = -27$ dyn/cm^2. The measured slope dL_p/dL_t (not shown) is -0.01326 which gives by employing Eq. (23) the local bending modulus $k_c = 1.41\times10^{-12}$ erg. The three indicated characteristic features of the experimental curve are $L_{t,0} = 5.92$ μm/s, $L_{t,\infty} = 1.58$ μm/s and $\Delta L_{t,e} = 100$ μm. From Eqs. (54) and (55) one obtains $\tau_s/\tau_p = 0.3004$ and $\alpha = 0.122$, respectively, which gives $k_r = 3.11\times10^{-12}$ erg, $\tau_s = 28$ s and $\tau_p = 93$ s. The solid line is the predicted curve obtained when the obtained material parameters are used in the integration of Eqs. (15) and (36) or by employing Eq. (39) (the two curves overlap). Materials and methods are as in Raphael and Waugh (1996)

obtain

$$\tau_s/\tau_p = \gamma(1-\gamma)/(1-\gamma+\delta)^2 \tag{54}$$

and

$$\alpha = \delta(1+\delta)/(1-\gamma+\delta)^2 \tag{55}$$

After having the value of the parameter α it is then possible by use of Eq. (25) to obtain the ratio k_r/k_c. As the bending modulus is obtained by the use of Eq. (23) and the measured dL_p/dL_t slope, both bending moduli are now known. Then from the initial slope Eq. (51)) one obtains τ_s and from Eq. (54) τ_p. An example is presented in Fig. 8. The exactly calculated time dependence of L_t obtained on the basis of the fitting parameters slightly deviates from the measurements at higher values of L_t. This may indicate that even in the case of smaller values of the parameter α the approximations may lead to slight inaccuracies in the predicted behavior (see also Fig. 4, case a). On the other hand, it is important to recognize that the experimental measurements themselves may be subject to instabilities, for example, in the chamber pressure, which might also contribute to the differences between theory and observation. In this regard it is relevant to note that the total change in aspiration pressure made to initiate tether formation was less than 1.0 mm H_20 (100 dyn/cm^2), and so it is quite possible that the deviation observed in Fig. 8 may be due to a small fluctuation in the experimental conditions.

Discussion

Observation of the mechanical behavior of thin membrane tubes (tethers) formed from giant phospholipid vesicles provides an effective means for determining the mechanical properties of the vesicle membrane. In the present report we have focused on the interpretation of tether formation experiments of long duration and the sensitivity of the process to the intrinsic membrane material properties as well as to the extrinsic geometry of the tethered vesicle. The present results establish guidelines for the applicability of certain algebraic approximations to the full numerical solution to the problem. We note in particular the importance of the parameter α (Eq. (25)), which must be small for simplifying limits to be taken. This parameter becomes large when the vesicle radius begins to approach the pipette radius. Previous analyses of long-term tether behavior were made under the assumption that the membrane tension (force resultant) was constant during the tether formation process and led to the prediction that the tether length should increase in time as the sum of an exponential plus a linear term (Raphael and Waugh 1996). For a tether formed at constant aspiration pressure, the membrane tension cannot remain absolutely constant because the tether radius increases very gradually as the tether grows. The dependence of the tension on vesicle radius is strongest when R_v approaches R_p. (In fact, the tension becomes infinite as R_v approaches R_p.) Thus, the conditions

under which the tension is approximately constant correspond to the situation where α is small. For typical values of the experimental parameters, the value of α should be less than 0.1 to ensure accuracy of the approximation within 5% for an experiment 200 s in duration. Although the value of α depends on several experimental parameters (Eq. (25)), this condition generally corresponds to a ratio of the vesicle radius to the pipette radius greater than 2.0. A surprising outcome of the present simulations was the fact that the range over which simplifying assumptions can be applied is increased when dissipative terms due to interleaflet friction and Stokes drag on the falling bead are included in the calculations.

A particular focus of the present analysis is the translocation of molecules between the leaflets of the bilayer that is thought to occur during tether formation. This translocation is the result of differences in leaflet stress associated with the deformation generated by alteration of the external forces. These stress differences are the consequence of the relative area expansivity deformation term of the elastic energy of the phospholipid vesicle (Evans 1974, 1980; Svetina et al. 1985). The increase of this relative area expansivity energy is particularly significant in tether pulling experiments because the difference between the areas of the layers increases proportionally to the tether length (Eq. (7)). For example, in a typical tethered vesicle (Waugh et al. 1992), a tether 500 μm in length corresponds to a difference in the area of each leaflet of approximately 0.5%, about 15% of the maximum area dilation which the membrane can support without rupture (Needham and Nunn 1990). These strains correspond to monolayer force resultants of $\simeq$0.5 mN/m, roughly five times larger than the mean tension in the membrane induced by the aspiration pressure in the pipette.

The relationship between the vesicle elasticity and transbilayer movement of phospholipid molecules is described here at the phenomenological level. It is asserted that the rate of the transbilayer movement is proportional to the derivative of the elastic energy of the vesicle (or free energy in the case of the externally stressed vesicle) with respect to the equilibrium area difference ΔA_0. The corresponding proportionality constant is introduced as a phenomenological parameter measuring the effectiveness of the relaxation process. It can be related to the equilibrium exchange time if it is assumed that the net transbilayer flow of phospholipids is based on the same stochastic events occurring in the membrane (Appendix I). Equilibrium exchange times corresponding to measured values of τ_p can be calculated via Eq. (I.10). Taking h=2.5 nm, $\bar{A}_0$=0.6 nm, kT=0.04×10^{-19} J and $k_r=4\times10^{-19}$ J, we find for a typical phospholipid membrane that the characteristic times τ_p for the equilibration of area differences are about an order of magnitude smaller than the corresponding equilibrium exchange times. Experimental results indicate that τ_p is of the order of minutes, meaning that the corresponding exchange times are of the order of 10 minutes. Measurements of the equilibrium exchange of molecules between the two membrane monolayers using molecular probes indicate that transmembrane lipid movement is a much slower process. Typical exchange half times in large vesicles like the ones used in tether formation experiments are approximately nine hours (Wimley and Thompson 1991). Such a large difference in time scales suggests that a membrane under stress may relax via pathways other than the process which is responsible for equilibrium molecular exchange, or by mechanisms other than simple diffusive transport. We note in particular that if lipid translocation occurs via localized "defects" in the membrane surface, that differences in lateral transport rate along the surface of the membrane to and from the defect may differ substantially when the transport is driven by differences in mechanical stress as opposed to gradients in concentration (Raphael and Waugh 1996).

An interesting consequence of allowing molecules to exhibit transmembrane movements is that the tether configuration becomes intrinsically unstable. Formerly it was established (Božič et al. 1992) that under the conditions of the tether experiment treated here, a stable vesicle configuration exists only if the ratio between the non-local and local bending constants exceeds a certain critical value which is approximately $k_r/k_c\cong1$. When molecules can freely traverse the bilayer, the non-local elasticity is dissipated. This corresponds formally to the condition that the value of k_r is zero, which is below the critical value for stability. Therefore, during tether growth, the system naturally tends to move away from equilibrium. This inherent instability of the process is manifested in a faster increase of the tether length L_t relative to the increase of the area difference (i.e. L_t^*) and thus in an increase of the difference $L_t-L_t^*$. Formally, this behavior is apparent in that the rate constant λ_2 (Eq. (42)) is positive. To maintain an equilibrium prior to forming a tether, the aspiration pressure was adjusted to keep the tether length constant (Eq. (18)), and so the system is made to appear stable because of adjustments made by the operator.

Prior to our understanding of the long-term dynamics of the tether formation process, estimates of the non-local bending modulus were obtained by attempting to establish equilibria at different tether lengths. In retrospect, it seems clear that some of the variability in the estimated values of k_r reported in those studies may be attributable to the relaxation of non-local area elasticity during the course of those measurements. More recent analyses (this report; Raphael and Waugh 1996) which account for the membrane dynamics provide a more reliable measure of the non-local modulus. Using the simple exponential plus linear approximation to the time course, Raphael and Waugh (1996) report a value for k_r of approximately 3.6×10^{-19} J and a ratio of k_r/k_c of approximately 3.0. This value is consistent with models relating the curvature elastic moduli to the area expansion modulus of the membrane in which it is assumed that the elastic resistance of the membrane to dilation and compression is distributed uniformly over the membrane cross-section (Waugh and Hochmuth 1987; Svetina and Žekš 1996). Within the uncertainty of the calculated parameters, the examples shown in the present report are consistent with this view.

Conclusion

This analysis establishes a rigorous framework for the interpretation of tether formation experiments of long duration. The present approach is general in nature and can be used with appropriate modifications to assess other mechanisms by which the area difference between the two membrane layers might change, such as the formation of non-bilayer structures, or an asymmetric transfer of phospholipid molecules to external compartments. In addition, we have explored the relationship between the apparent rate of mechanically-driven lipid translocation and the corresponding half times for lipid exchange. An important conclusion of the work is that the apparent half times for mechanically-driven lipid translocation are nearly two orders of magnitude smaller than half times for lipid exchange measured using chemical probes. This conclusion has important implications for fundamental mechanisms underlying the generation and maintenance of lipid asymmetry in living cells.

Acknowledgements This work was supported by The Ministry of Science and Technology of the Republic of Slovenia under Grant J3-7033-381, under the US-Slovene Grant DHHS 95–150, and in part by the National Science Foundation under Grant No. PHY94-07194 (participation of S. S. in the Research Program in Biomembranes). Additional support was obtained from the US Public Health Service under NIH grant No. HL31524.

Appendix I

Relationships corresponding to a simple diffusive mechanism for lipid translocation

In general the exchange of phospholipid molecules between the two membrane layers can occur as a consequence of a stochastic process induced by the thermal energy. Through such a process the mechanical energy stored in the system can also be dissipated. Here we present some basic relationships.

We consider a vesicle with a given shape which means that the areas of the external layer (A^{out}) and of the internal layer (A^{in}) are constant. The mean number of molecules which per unit time "flip" from the outer to the inner layer can be assumed to be proportional to the number of molecules in this layer, N^{out}, and to the proportionality constant w_{oi} which is the probability for a flip to occur in a unit of time. The number of molecules which per unit time "flop" from the inner layer to the outer layer is correspondingly proportional to the number of molecules in the inner layer, N^{in}, and the probability per unit time w_{io}. Then the numbers of molecules in the outer and the inner layer change in time as

$$\frac{dN^{out}}{dt} = -w_{oi}\,N^{out} + w_{io}\,N^{in} \tag{I.1}$$

$$\frac{dN^{in}}{dt} = w_{oi}\,N^{out} - w_{io}\,N^{in}\,. \tag{I.2}$$

At equilibrium, i. e. when both layers are unstretched, the numbers N^{out} and N^{in} do not vary in time. Their ratio is given by the ratio of the probability constants at equilibrium, which are in turn proportional to the ratio of the equilibrium areas of the two layers. This last condition ensures that the phospholipid area densities in the equilibrium are equal:

$$\frac{N^{out}}{N^{in}} = \frac{w_{io,eq}}{w_{oi,eq}} = \frac{A^{out}}{A^{in}}\,. \tag{I.3}$$

In nonequilibrium, i. e. when the two layers are differently stretched, the ration between the rate constants is equal to

$$\frac{w_{io}}{w_{oi}} = \frac{A^{out}}{A^{in}}\,e^{-\Delta\mu/kT}\,, \tag{I.4}$$

where $\Delta\mu$ is the difference between the chemical potentials (per molecule) of the outer and the inner layer, k is Boltzmann constant and T temperature.

The chemical potential difference $\Delta\mu$ in Eq. (I.4) can be obtained as the derivative of the vesicle elastic energy (Eq. (2)) (or of the free energy in the case of the externally stressed vesicle) by $N^{out}-N^{in}$:

$$\Delta\mu = dW_{el}/d(N^{out}-N^{in})\,, \tag{I.5}$$

which gives by taking into account Eq. (3)

$$\Delta\mu = -\frac{k_r}{A_0\,h^2}\,(\Delta A - \Delta A_0)\,\overline{A}_0\,. \tag{I.6}$$

By subtracting Eq. (I.2) from Eq. (I.1) we get

$$\frac{d(N^{out}-N^{in})}{dt} = -2\,w_{oi}\,N^{out} + 2\,w_{io}\,N^{in}\,. \tag{I.7}$$

The probability constant w_{io} can be expressed in terms of w_{oi} (Eq. (I.4)) and inserted into Eq. (I.7). Then, assuming $\Delta\mu \ll kT$, and keeping only linear terms in ΔA and ΔA_0 (which is a linear function of $N^{out}-N^{in}$ (Eq. (3)), we obtain

$$\frac{d\Delta A_0}{dt} = \frac{1}{\tau}\left(\frac{\overline{A}_0\,k_r}{kT\,h^2}+1\right)(\Delta A - \Delta A_0)\,. \tag{I.8}$$

Here,

$$\tau = 1/2\,w_{oi} \tag{I.9}$$

is the equilibrium exchange time. We have also taken $N^{out} \cong N^{in} \cong N$, i. e. the average number of molecules in a leaflet, and $A_0^{out} \cong A_0^{in}$ in all cases where these quantities do not appear as differences between themselves.

Equation (I.8) describes the relaxation of the distribution of the phospholipid molecules between the two membrane layers due to the flip-flop mechanism. The relaxation time τ_p for this process is given by

$$\frac{1}{\tau_p} = \frac{1}{\tau}\left(\frac{\overline{A}_0\,k_r}{kT\,h^2}+1\right). \tag{I.10}$$

Thus, using experimentally determined values for τ_p, the corresponding exchange time τ can be obtained for the case that the mechanical relaxation occurs by a simple diffusive mechanism.

References

Bo L, Waugh RE (1989) Determination of bilayer membrane bending stiffness by tether formation from giant, thin-walled vesicles. Biophys J 55: 509–517

Božič B, Svetina S, Žekš B (1997) Theoretical analysis of the formation of membrane microtubes on axially strained vesicles. Phys Rev E 55: 5834–5842

Božič B, Svetina S, Žekš B, Waugh R (1992) Role of lamellar membrane structure in tether formation from bilayer vesicles. Biophys J 61: 963–973

Evans EA (1974) Bending resistance and chemically induced moments in membrane bilayers. Biophys J 14: 923–931

Evans EA (1980) Minimum energy analysis of membrane deformation applied to pipet aspiration and surface adhesion of red blood cells. Biophys J 30: 265–284

Evans E, Yeung A (1994) Hidden dynamics in rapid changes of bilayer shape. Chem Phys Lipids 73: 39–56

Evans EA, Yeung A, Waugh RE, Song J (1992) Dynamic coupling and nonlocal curvature elasticity in bilayer membranes. In: Lipowsky R, Richter D, Kremer K (eds) The structure and conformation of amphiphilic membranes. Springer Proc Phys, vol 66. Springer, Berlin Heidelberg New York, pp 148–153

Heinrich V, Svetina S, Žekš B (1993) Nonaxisymmetric vesicle shapes in a generalized bilayer-couple model and the transition between oblate and prolate axisymmetric shapes. Phys Rev E 48: 3112–3123

Helfrich W (1973) Elastic properties of lipid bilayers: theory and possible experiments. Z Naturforsch 28c: 693–703

Hochmuth RM, Shao J, Dai J, Sheetz MP (1996) Deformation and flow of membrane into tethers extracted from neuronal growth cone. Biophys J 70: 358–369

Landau LD, Khalatnikhov IM (1954) Ob anomalnom pogloshchenii zvuka vblizi tochek fazovovo perehoda vtorovo roda. Dokl Akad Nauk SSSR 96: 469–472

Miao L, Seifert U, Wortis M, Döbereiner HG (1994) Budding transitions of fluid-bilayer vesicles: The effect of area-difference elasticity. Phys Rev E 49: 5389–5407

Needham D, Nunn RS (1990) Elastic deformation and failure of lipid bilayer membranes containing cholesterol. Biophys J 58: 997–1009

Raphael RM, Waugh RE (1996) Accelerated interleaflet transport of phosphatidylcholine molecules in membranes under deformation. Biophys J 71: 1374–1388

Seifert U, Langer SA (1993) Viscous modes of fluid bilayer membranes. Europhys Lett 23: 71–76

Svetina S, Žekš B (1989) Membrane bending energy and shape determination of phospholipid vesicles and red blood cells. Eur Biophys J 17: 101–111

Svetina S, Žekš B (1996) Elastic properties of closed bilayer membranes and the shapes of giant phospholipid vesicles. In Lasic DD, Barenholz Y (eds) Handbook of nonmedical applications of liposomes, vol I. CRC Press, Boca Raton New York London Tokyo, pp 13–42

Svetina S, Brumen M, Žekš B (1985) Lipid bilayer elasticity and the bilayer couple interpretation of red cell shape transformations and lysis. Stud Biophys 110: 177–184

Waugh RE, Bauserman RG (1995) Physical measurements of the bilayer-skeletal separation forces. Ann Biomed Eng 23: 308–321

Waugh RE, Hochmuth RM (1987) Mechanical equilibrium of thick, hollow, liquid membrane cylinders. Biophys J 52: 391–400

Waugh RE, Song J, Svetina S, Žekš B (1992) Monolayer coupling and curvature elasticity in bilayer membranes by tether formation from lecithin vesicles. Biophys J 61: 974–982

Wimley WC, Thompson TE (1991) Transbilayer and interbilayer phospholipid exchange in dimyristoylphosphatidylcholine/dimyristoylphosphatidylethanolamine large unilamellar vesicles. Biochemistry 30: 1702–1709